Available online at www.sciencedirect.com
ScienceDirect
Journal of Photochemistry and Photobiology A: Chemistry 195 (2008) 357–363
Journal of Photochemistry and Photobiology A:Chemistry
www.elsevier.com/locate/jphotochem

Preparation and photoelectric performance of ITO/TiO_2/CdS composite thin films

Yu-juan Chi [a], Hong-gang Fu [a,*], Le-hui Qi [b], Ke-ying Shi [b], Heng-bin Zhang [b], Hai-tao Yu [b]

[a] *Department of Applied Chemistry, Harbin Institute of Technology, Harbin 150001, PR China*
[b] *School of Chemistry and Materials Science, Heilongjiang University, Harbin 150080, PR China*

Received 19 April 2007; received in revised form 2 November 2007; accepted 7 November 2007
Available online 17 November 2007

Abstract

ITO/TiO_2/CdS composite thin films were successfully prepared by electrodeposition of CdS on ITO/TiO_2 substrate. The prepared ITO/TiO_2/CdS thin films were characterized in detail by X-ray diffraction, surface photovoltage, and scanning electronic microscopy techniques. The results indicated that the deposited CdS layer with about 1:1 stoichiometry of Cd and S distributes not only on the surface with cauliflower-like structure but also the TiO_2 film interior and even in the immediate proximity to the surface of ITO substrate. The UV–vis absorption spectrum results suggested that the absorption peak of the ITO/TiO_2/CdS film shifts from the ultraviolet region to the visible region in comparison to that of the ITO/TiO_2 film. Furthermore, by the photocurrent–potential behavior and incident monochromatic photon to current conversion efficiency measurements, it can be also noted that the deposited ITO/TiO_2/CdS thin films possess higher photoelectric conversion efficiency than the ITO/TiO_2 films. The sensibilization of TiO_2 with CdS can effectively improve steady photocurrent. Therefore, the modification of CdS for ITO/TiO_2 can strongly ameliorate the photoelectric capability of ITO/TiO_2 thin film, and the prepared ITO/TiO_2/CdS thin films were expected to possess more excellent photoelectrochemical performance than the ITO/TiO_2 films.

Keywords: Electrodeposition; Titanium dioxide; Cadmium sulfide; Photocurrent response

1. Introduction

Semiconductor film materials have very wide applications in photovoltaic conversion techniques. However, for a single semiconductor film, the existence of a quick back electron transfer, *i.e.*, the so-called charge recombination, makes it difficult to obtain high photovoltaic conversion efficiency [1]. The combination of two or more semiconductors with appropriate energy levels, which can produce a long-distance charge-separated state with electrons and holes at sites far from each other, is a very effective approach to suppress the back electron transfer [2]. For example, Nasr and co-workers investigated the TiO_2/CdS, ZnO/CdS, TiO_2/CdSe, and SnO_2/CdSe systems and observed an obvious photocurrent improvement for the coupled films relative to the single semiconductor materials [3]. Other investigations for the TiO_2/CdS, ZnO/Bi_2S_3, and TiO_2/PbS systems by Vogel also indicated that the combination of a narrow-band-gap semiconductor with a broad-band-gap one can effectively separate the excited electrons and accelerate the transfer process of the photogenerated electrons [4]. For improving the performance of TiO_2 thin film, a widely mentioned narrow-band-gap material, such as CdS, Bi_2S_3 and CdSe, *etc.*, have been used to couple with TiO_2 film [2–4]. Especially, considering that CdS is a direct band-gap semiconductor material with band-gap of 2.43 eV and its energy levels can match with those of TiO_2 [2], one reasonably expects that the sensibilization of TiO_2 film with CdS can effectively enhance the conversion of sunlight and improve the photoelectric performance of TiO_2 film electrodes. Therefore, the semiconductor combination of TiO_2 with CdS were investigated widely [2,5–19], such as the combination of *in situ* prepared CdS particles with a highly porous nanocrystalline TiO_2 electrode [9], the deposition of CdS microcrystals onto a TiO_2 semiconductor [10], the quantum-sized CdS and TiO_2 particles films [2], CdS–TiO_2 particle film electrodes [11],

* Corresponding author. Tel.: +86 451 86608458.
E-mail address: fuhg@vip.sina.com (H.-g. Fu).

1010-6030/$ – see front matter © 2007 Elsevier B.V. All rights reserved.
doi:10.1016/j.jphotochem.2007.11.002

TiO_2–CdS composite nanotubes [12], *et al.* However, it should be noted that the TiO_2/CdS films prepared in previous studies were often used as catalyst to decompose organic compounds [18,19].

In a pioneer work on the TiO_2/CdS composite film, Bai and co-workers studied the photosensitization of TiO_2 nanoparticle thin film electrodes by CdS nanoparticles by means of the surface photovoltage spectra (SPS) technique, in which they identified that by the CdS nanoparticle sensitization for TiO_2/CdS composite film the slow photocurrent response disappears and the steady-state photocurrent increases obviously, suggesting the photosensitization to be very effective in decreasing the effect of surface states on photocurrent response [20]. In their another work [21], they also confirmed that for the CdS sensitized TiO_2 thin film electrode the semiconductor sensitization is an efficient way to decrease the influence of surface state on the charge separation and can improve the photocurrent response intensity. Very recently, a densely packed TiO_2 thin film onto an indium-doped-tin oxide (ITO) substrate was synthesized at room temperature by chemical deposition, and subsequently, a CdS thin film was deposited onto the pre-deposited TiO_2 film by a doctor blade route (powder of CdS was obtained from chemical deposition) [22]. However in the experiment, only the *I–V* property was given.

Furthermore, as another two typical examples, the TiO_2/CdS films were successfully prepared by sol–gel [23] and chemical bath deposition (CBD) [24] techniques. However, unfortunately, the results indicate that it is very difficult for the two conventional methods to obtain uniform distribution of nanocrystallite CdS on TiO_2, and this is very unfavorable for the improvement of the photoelectrochemistry properties of CdS/TiO_2 film. Considering the advantages of the electrodeposition technique, Flood and co-workers successfully prepared the ITO/TiO_2/CdS composite film followed by an investigation regarding its band-gaps [11], which suggested that the TiO_2/CdS sandwich films possess potential applications in regenerative photoelectrochemical cells. They also found that the electrodeposition of CdS on ITO/TiO_2 using sulfur and $CdCl_2$ in DMSO results in poor morphologies [11], which may affect the performance of the prepared TiO_2/CdS film electrodes. Furthermore, previous studies indicated that for the chemical deposit and sol–gel methods the preparation steps are very inconvenient and the preparation processes need a heat treatment at 200–400 °C for obtaining a fine crystallinity [22,25]. Also, some impurities are very easy to be deposited into the samples in the treatment, leading to the performance decrease of thin films [26]. However, fortunately, some investigations implied that these disadvantages can be effectively avoided by the use of the electrodeposition technique [27–29].

Therefore, in the present study, the ITO/TiO_2/CdS composite thin films were prepared by electrodeposition of CdS on high porosity ITO/TiO_2 substrate prepared by mixing TiO_2 nanoparticles and colloid. The preparation method can effectively improve the distribution of CdS around TiO_2 nanoparticles and the porosity of the thin film. Also, the prepared ITO/TiO_2/CdS composite thin films can effectively capture the visible light and quickly transfer the photogenerated electrons into the TiO_2 conduction band, and finally, the sensitization of CdS on ITO/TiO_2 strongly ameliorate the photoelectric performance of the ITO/TiO_2 films.

2. Experimental details

2.1. Preparation of nanostructured ITO/TiO_2 thin films

For obtaining nanostructured TiO_2 thin films with high performance, a film preparation technique including the mix of TiO_2 nanoparticles and colloid was employed. TiO_2 nanoparticles were prepared by the hydrothermal method [30]. $Ti(OBu)_4$ and isopropyl alcohol solution were slowly dropped into nitric acid aqueous solution under vigorous stirring, and subsequently, the formed solution was heated for 4 h at 80 °C and further treated with ammonia liquor to adjust its pH value. In succession, the solution was put inside a hydrothermal reaction kettle and kept for 8 h at 180 °C. The turbid solution taken from the kettle was washed with water and ethanol for several times, and then, the wet TiO_2 nanoparticles were obtained by centrifugation. Finally, the wet TiO_2 nanoparticles were shifted to an agate mortar and mixed with a slight amount of polyethylene and acetylacetone followed by a grinding to form a paste with better distribution of TiO_2 nanoparticles.

TiO_2 colloid was prepared by the sol–gel technique [31]. A small quantity of acetylacetone and polyethylene glycol was added into the absolute ethanol solution including $Ti(OBu)_4$ dropwise under vigorous stirring. The solution obtained was continuously stirred for 2 h followed by the addition of redistillation water to form TiO_2 colloid.

The prepared TiO_2 nanoparticle paste was mixed with TiO_2 colloid at definite volume ratios (3:1) followed by violently ultrasonic oscillation for 2 h. In succession, a cleaned ITO glass substrate with a sheet resistance of 15 $\Omega\,cm^{-2}$ was immerged into the mixed solution for 1 min. And then, the glass substrate was upward drawn slowly to form an as-dipped film. Subsequently, the as-synthesized TiO_2-coated ITO glass was calcinated at 450 °C for 1 h to establish the electrical contact among the nanoparticles and form a ITO/TiO_2 nanostructured film. Finally, a silver wire was fixed on the film using conducting resin and the free area of the film was covered with epoxy resin to form a film electrode with the exposed area of 1.0 cm^2.

2.2. Electrodeposition of CdS on ITO/TiO_2 thin film

The electrodeposition of CdS on the ITO/TiO_2 substrate was performed potentiostatically using the cathodic electrodeposition method in a three-electrode configuration with the prepared ITO/TiO_2 thin film as working electrode, a Pt sheet as counter electrode, and an Ag/AgCl as reference electrode. The electrodeposition bath was an aqueous solution containing $CdCl_2$ (0.1 mol/L) and $Na_2S_2O_3$ (0.01 mol/L) and was adjusted to pH 2.0 with a dilute HCl solution. The cathode potential was kept at −1.0 V with respect to the Ag/AgCl reference electrode, and the electrodeposition proceeded at a constant temperature of 40 °C for 20 min.

2.3. Characterization

The X-ray diffraction (XRD) patterns were obtained by a Japan Rigaka TV-5400 X-ray diffractometer using Cu Kα radiation (λ = 0.15406 nm). Scanning electronic microscopy (SEM) (Philips XL-30-ESEM-FEG Scanning Microscope operating at 20 kV) was used to evaluate the surface morphology, composition, and thickness of the prepared films. The ultraviolet–visible (UV–vis) absorption spectra were recorded on a Japan Shimadzu UV-3100 spectrometer. The SPS measurement was carried out with a home-built apparatus that has been described elsewhere [32,33]. Monochromatic light is obtained by passing light from a 500 W xenon lamp (CHFXQ500W, Global Xenon Lamp Power, made in China) through a double-prism monochromator (Hilger and Watts, D300, made in England). A lock-in amplifier (SR540, made in USA), synchronized with a light chopper (SR540, made in USA), was employed to amplify photovoltage signals. The measurement was performed in a photovoltage cell consisting of two ITO quartz glass electrodes. The raw SPS data were normalized using illuminometer (Zolix UOM-1S, made in China).

2.4. Electrochemical and photoelectrochemical measurement

The electrochemical and photoelectric performance experiments were performed by a standard three electrode system in a quartz cell, in which the prepared ITO/TiO_2 and ITO/TiO_2/CdS thin films were used as working electrode (working area is 1 cm^2), a platinum plate as counter electrode, and a saturated calomel electrode (SCE) as reference electrode. Note that all potentials reported on the electrochemical and photoelectrochemical measurement were measured against SCE. The linear scanning voltammetry experiments were performed in an aqueous solution containing K_2SO_4 of 0.1 mol/L by the BAS/100B potentiostat. Furthermore, the BAS/100B potentiostat, together with the SPB300 monochromator and a high-pressure Xe lamp of 150 W giving an irradiation area of 0.2 cm^2, was also used to determine the photocurrent action spectra of the prepared ITO/TiO_2 and ITO/TiO_2/CdS thin film electrodes in aqueous solution consisting of 1.0 mol/L KI [34] and 0.1 mol/L K_2SO_4. In this study, the intensity of light was determined by a radiometer and the wavelength scanning ranges between 600 and 300 nm. The photocurrent–time behaviors of the prepared ITO/TiO_2 and ITO/TiO_2/CdS thin film electrodes were described with a hand-chopped light in an aqueous solution consisting of 1.0 mol/L KI and 0.1 mol/L K_2SO_4 under potentiostatic condition (287 mV).

3. Results and discussion

3.1. Thin film structure

The XRD patterns of ITO/TiO_2 and ITO/TiO_2/CdS thin films were presented in Fig. 1(a) and (b), respectively. Fig. 1(a) clearly shows the typical XRD pattern of an anatase TiO_2 structure. These broad diffraction peaks imply very small particle sizes of TiO_2 in ITO/TiO_2 thin film. By means of the Scherrer equation and (1 0 1) diffraction peak values, an average particle size

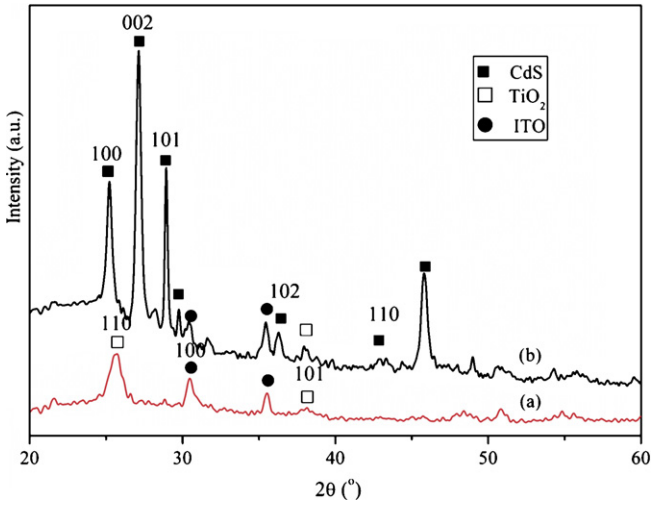

Fig. 1. XRD patterns of ITO/TiO_2 films (a) and ITO/TiO_2/CdS films (b).

of 12.0 nm is suggested. The formation of nanocrystallite CdS on ITO/TiO_2 electrodes can be confirmed by the XRD pattern shown in Fig. 1(b). Besides the diffraction peaks coming from the ITO/TiO_2 substrate, another three strong diffraction peaks are observed at $2\theta = 24.93°$, 26.91°, 28.71°, which can be indexed as (1 0 0), (0 0 2), and (1 0 1) diffraction peaks of the hexagonal phase CdS, respectively. The pronounced peaks from the (0 0 2) crystal face suggest a certain preference for the crystallographic orientation of CdS with its *c*-axis perpendicular to the substrate, although the ITO/TiO_2 substrate has a rough surface with a random crystallographic orientation. The experimental results are in good agreement with previous predictions about CdS–TiO_2 particulate films [35]. Furthermore, owing to the existence of diffraction peaks at $2\theta = 29.89°$ and $2\theta = 46.56°$, we think that there is a small amount of CdS with cubical phase in the sample. It can be noted that CdS deposited at 40 °C possesses a good crystallinity even if no high temperature calcination is used. However, when the chemical deposition technique is adopted, a good crystallinity of CdS can be obtained at the temperature of more than 300 °C [22].

Fig. 2(a)–(c) give the SEM images of the ITO/TiO_2 and ITO/TiO_2/CdS composite thin films. The SEM micrograph in Fig. 2(a) clearly displays that the film is rather rough and possesses uniform spheral TiO_2 grains with particle size of about 12.4 nm, being consistent with the XRD results. The SEM image (Fig. 2(b)) of the ITO/TiO_2/CdS thin film shows that the deposited CdS layer presents cauliflower-like appearance (about 54.2 nm), and the grain size of CdS is about 10 nm.

The inset of Fig. 2(b) shows the energy dispersive X-ray (EDX) analysis result of the ITO/TiO_2/CdS thin film surface, which strongly demonstrates the existence of Cd and S on the substrate surface. Quantitative analysis result suggested an atomic composition of 50.4% Cd and 49.6% S, being close to 1:1 stoichiometry. Therefore, the distribution of Cd and S are homogeneous in composition at different positions of the film surface. For clearly describing the distribution of CdS particles in the prepared films, we performed an energy spectrum characterization and a SEM analysis for the cross sections of the ITO/TiO_2/CdS thin films. The EDX data show that the CdS particles distribute

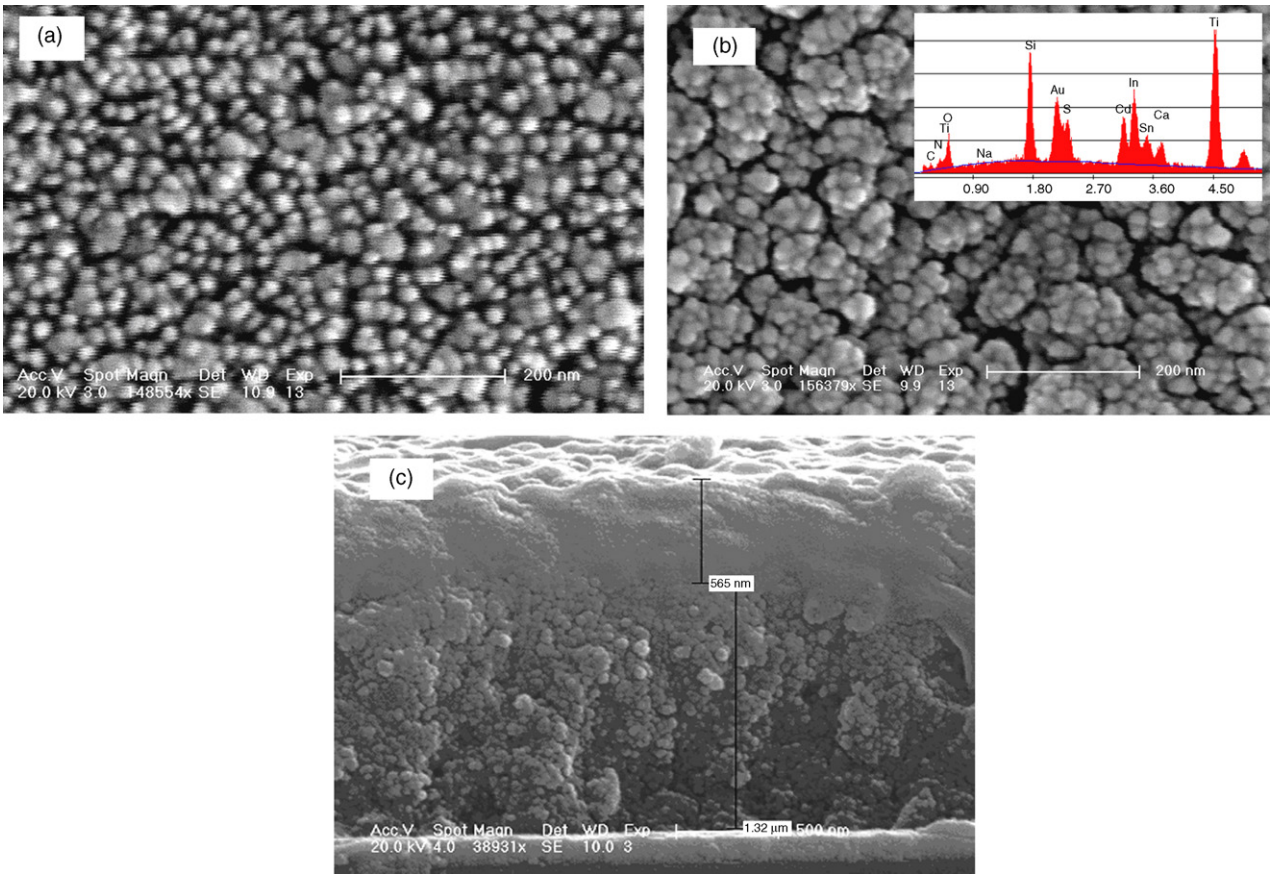

Fig. 2. SEM photographs of ITO/TiO_2 (a), ITO/TiO_2/CdS (b), and the cross section of ITO/TiO_2/CdS (c). The ITO/TiO_2 films were calcined at 400 °C for 1h and the CdS particles were deposited at the potential of −1.0 V (*vs.* Ag/AgCl) for 20 min. The inset figure is EDX diagram of the ITO/TiO_2/CdS.

not only on the surface but also the TiO_2 film interior and even reach the surface of the ITO substrate. The distribution can be attributed to the electrodeposition process, in which Cd^{2+} and S^{2-} formed from $S_2O_3{}^{2-}$ in the acidic electrolyte easily diffuse into the gaps and holes of TiO_2 and some of them can reach the surface of the ITO substrate followed by the reactions of Cd^{2+} with S^{2-} to CdS particles, resulting in the coated TiO_2 particles by CdS. Finally, after the holes and gaps of the TiO_2 particle film are filled, the deposition of CdS particles proceeds on the surface of the TiO_2 film to form ITO/TiO_2/CdS composite film with cauliflower-like morphology. In the formed composite film, CdS uniformly distributes around the TiO_2 particles, and the compact combine forms a heterojunction between TiO_2 and CdS.

As can be seen from the SEM image (Fig. 2(c)) of the ITO/TiO_2/CdS thin film cross section, the CdS deposit layer with the thickness of 1.88 μm consists of the loose and compact layers, which can be attributed to the deposition of CdS in the holes and gaps of the TiO_2 particles and on the surface of the TiO_2 film, respectively. The results suggest the thicknesses of the loose and compact layers to be 1.32 and 0.56 μm, respectively.

3.2. UV–vis absorption and SPS characteristics

The UV–vis absorption spectra of the ITO/TiO_2 and ITO/TiO_2/CdS thin films were showed in Fig. 3. The absorption of the ITO/TiO_2 film was found to locate at the ultraviolet region, and the absorption wavelength is less than 380 nm. However, it is obvious that the absorption edge of the deposited ITO/TiO_2/CdS thin film is strongly expanded to visible light region, as can be seen from Fig. 3 that a strong and wide absorption was observed from about 400 to 500 nm, strongly suggesting that the sensibilization of CdS particles for ITO/TiO_2 film can availably expand the photoabsorption range of the ITO/TiO_2 film. Furthermore, in this study, the observed absorption band edge of 485 nm of the prepared ITO/TiO_2/CdS films suggests a strong blue shift by

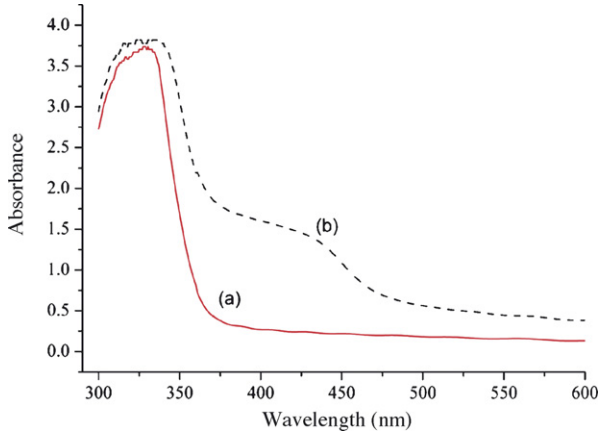

Fig. 3. Absorption spectra of ITO/TiO_2 (a) and ITO/TiO_2/CdS (b) thin films.

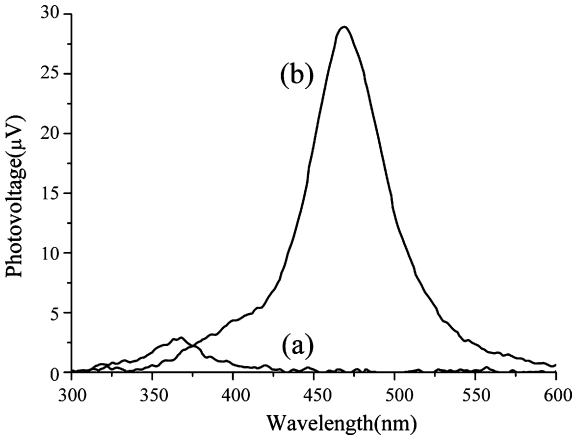

Fig. 4. SPS responses of ITO/TiO_2 (a) and ITO/TiO_2/CdS (b) thin films.

comparison with the reported initial wavelength of 514.5 nm of the bulk wurtzite CdS intrinsic absorption [2], indicating a very obvious size quantization effect of the nanoparticles.

Fig. 4 shows the SPS responses of the ITO/TiO_2 and ITO/TiO_2/CdS thin films. The strong SPS peaks of the ITO/TiO_2 and ITO/TiO_2/CdS thin film electrodes were observed at about 350 nm, as can be seen from Fig. 4(a), which were attributed to the electron transition from valence to conduction bands of TiO_2 ($O_{2p} \rightarrow Ti_{3d}$). But for the SPS responses of the ITO/TiO_2/CdS thin films, except for the signal peak at 350 nm, the intensity of which is weakened by comparison with that of the ITO/TiO_2 thin film and resulting from the cover of CdS on TiO_2, we found a new peak at 475 nm with very strong intensity. The peak can be attributed to the photogenerated electron transition from the conduction band of CdS to that of TiO_2 with the holes accumulated at the CdS particles. Because of smaller energy gap (2.4 eV *vs.* 3.2 eV for CdS and TiO_2, respectively) and higher conduction band location (−0.8 eV *vs.* −0.4 eV for CdS and TiO_2, respectively) [6], the photogenerated electrons from CdS can be quickly injected into the conduction bands of TiO_2. Note that the mentioned energy gap and conduction band location are relative to the normal hydrogen electrode (NHE). The quick transfer can effectively restrain the electron–hole recombination and leads to very strong surface photovoltage signals. The above-mentioned photoabsorption and photovoltage characteristics suggest that the ITO/TiO_2/CdS thin film possesses more excellent photoelectrochemistry performance than the ITO/TiO_2 thin film.

3.3. Photoelectric performance of the ITO/TiO_2/CdS composite films

Fig. 5(a) and (b) shows the photocurrent–potential behaviors of the ITO/TiO_2 and ITO/TiO_2/CdS thin film electrodes, respectively. From Fig. 5(b), we observe a higher cathodic current and it can be attributed to the electrolysis of water and extremely small anodic dark current with microampere order of magnitude. However, under illumination, we can observe a large increase in current. By comparing the dark current with the photocurrent under illumination, we can know that the dark current is relatively very low to the photocurrent under illumination. Thereby, we can ignore the dark current in our study and consider the current under illumination as observed photocurrent. This is in good agreement with previous observation [21]. Furthermore, we also found that the photocurrent of the ITO/TiO_2/CdS film electrode gradually increases with the increase of anodic polarization potential and finally approaches a constant when the polarization is higher than 200 mV. But considering that in the process the photocurrent increases only 0.06 mA (from 0.16 mA at −400 mV to 0.22 mA at 400 mV), we can reasonably expect that the effect of bias voltage on photovoltaic conversion is very slight.

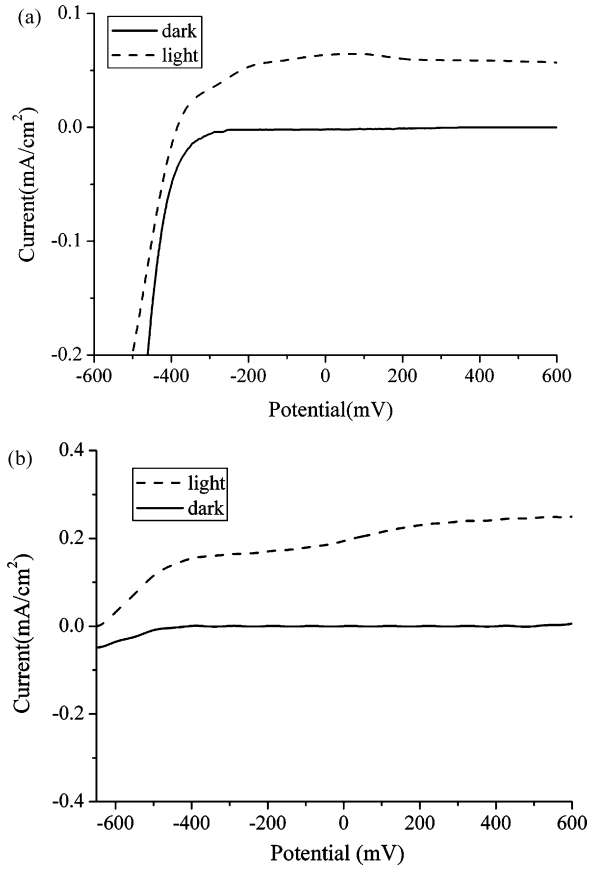

Fig. 5. Photocurrent–potential behaviors of ITO/TiO_2 (a) and ITO/TiO_2/CdS (b) thin film electrodes. The experiment was performed in a solution with 1.0 mol/L KI and 0.1 mol/L K_2SO_4 upon dark and illumination with Xenon lamp (150 W). The electrode potentials are given *vs.* SCE.

It can also be noted from Fig. 5(a) and (b) that the photocurrent of the ITO/TiO_2/CdS film electrode is obviously higher than that of the ITO/TiO_2 film electrode. As an example we can note that at the potential of 200 mV the photocurrents are 0.22 and 0.06 mA/cm^2 for the ITO/TiO_2/CdS and ITO/TiO_2 film electrodes, respectively. It can be known from previous discussion that the CdS particles in the prepared CdS/TiO_2/ITO composite film with large numbers of heterojunctions are uniformly distributed around TiO_2 grains. Under illumination with the light wavelength less than 500 nm, the electrons of CdS are excited, as shown in Fig. 6. Because the conduction band energy levels of CdS match with those of TiO_2, the excited electrons from

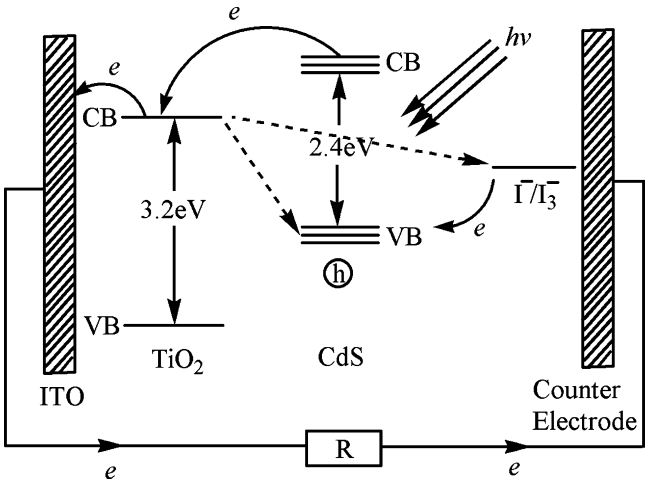

Fig. 6. Schematic electron energy and photocurrent generation mechanism diagram of CdS/TiO_2 semiconductors in electrolyte.

CdS can quickly be injected into the conduction band of TiO_2 followed by quick transport to the counter electrode *via* external circuit while the holes reside on the CdS. Finally, the electron cycle is finished *via* the redox couple $I^-/I_3{}^-$. It seems that the coupling of CdS and TiO_2 can effectively improve the separate of electron and hole pairs, resulting in a higher photocurrent of ITO/TiO_2/CdS relative to ITO/TiO_2.

Fig. 7 shows the photocurrent action spectra (the incident monochromatic photon to current conversion efficiency (IPCE (%)) *vs.* various incident lights of different wavelength) of the ITO/TiO_2 and ITO/TiO_2/CdS film electrodes. Short-circuit photocurrents are measured at various excitation wavelengths for each electrode and IPCE (%) was determined from the expression [36]

$$\text{IPCE}\ (\%) = \frac{1.24 \times 10^3 (\text{W nm/A}) \times i_{\text{SC}}(\mu\text{A/cm}^2)}{\text{Wavelength(nm)} \times I_{\text{nc}}(\text{W/m}^2)} \times 100$$

where i_{sc} is the short-circuit current and I_{nc} the incident light intensity. From Fig. 7, we can observe a very obvious photocurrent response at the wavelength range from 400 to 550 nm, which can clearly identify that the sensitization of CdS on the ITO/TiO_2

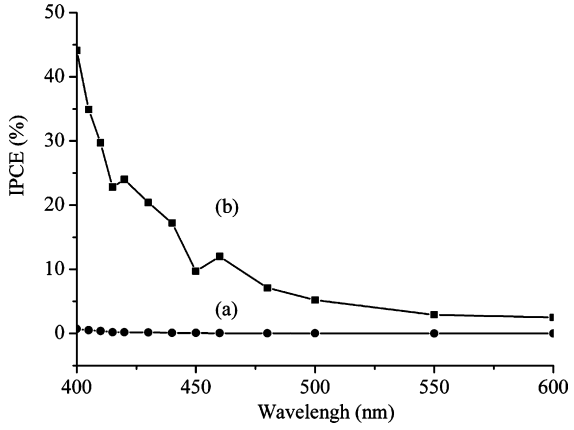

Fig. 7. Photocurrent action spectra of ITO/TiO_2 (a) film electrode and ITO/TiO_2/CdS (b) film electrodes in the solution of 1.0 mol/L KI and 0.1 mol/L K_2SO_4 at the electrode potential of 0 V.

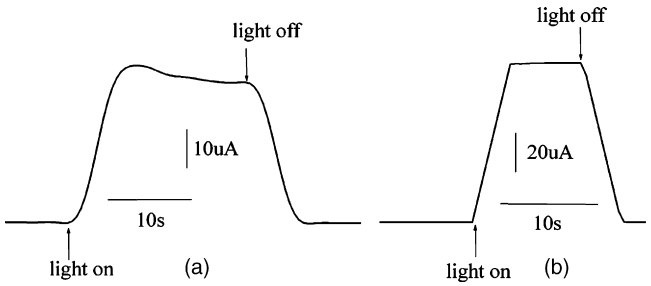

Fig. 8. Transient photocurrent action spectra of ITO/TiO_2 (a) and ITO/TiO_2/CdS (b) electrodes at 0.30 V bias voltages and upon illumination with white light of 150 W. The experiments were performed in a 1.0 mol/L KI and 0.1 mol/L K_2SO_4 solution.

thin film can broaden the response band to visible light region. The result is accordant with the observed absorption characteristics above. The response can be understood by the injection of photogenerated electrons from CdS into the conduction band of TiO_2. Furthermore, we also observed that the IPCE (%) are 45 and 5% upon irradiation with the light wavelengths of 400 and 500 nm, respectively. The result is in accord with previous investigation [37].

To better estimate the restrainability for the carrier recombination triggered by the CdS sensitization on the ITO/TiO_2, the transient photocurrent responses of several on–off cycles of the prepared ITO/TiO_2/CdS and ITO/TiO_2 film electrodes under illumination were recorded. Some representative traces are shown in Fig. 8. The results indicated that for the ITO/TiO_2 film electrodes the photocurrent increases slowly at the moment of illumination and decreases tardily after reaching a value, and finally, keep a constant current value after about 8 s. This can be understood from the capture of surface states and the release of electrons. At the beginning of illumination, the photogenerated electrons are first injected into the surface states with shallow energy level followed by the quick transfer to the surface states with deep energy level. When the surface states with deep energy level are fully filled, the capture and release of electrons on the shallow energy level surface states reach a homeostasis, *i.e.*, the photocurrent keeps a constant value.

However, by comparing Fig. 8(a) with Fig. 8(b), we can note that for the ITO/TiO_2/CdS film electrode the photocurrent increases quickly at the initial moment of illumination and reaches a steady state after about 2 s. Furthermore, it can found that the steady photocurrent of the ITO/TiO_2/CdS film electrode is higher than that of the ITO/TiO_2 film electrode. Also, it can be noted from Fig. 8(a) and (b) that when the ITO/TiO_2 film electrode is illuminated, the photocurrent increases slowly and reaches a maximum value after 3 s followed by a slow decrease to a steady photocurrent. However, for the ITO/TiO_2/CdS film electrode, the photocurrent increases quickly upon illumination and finally reaches a steady value after 2 s. In the process, no any decrease is observed. This result implies that plentiful surface states and defects should exist on the surface of ITO/TiO_2, which can effectively trap the photogenerated electrons and lead to the combination of the photogenerated electrons and the slow increase in photocurrent. However, the deposition of CdS on ITO/TiO_2 can decrease the surface state density and defect and

effectively restrains the capture for the photogenerated electrons. Therefore, the photogenerated current can increase quickly and finally get to a higher steady value. These results indicate that the sensitization of CdS on the ITO/TiO_2 film can effectively restrain the capture for the photogenerated electrons and makes the photocurrent reach a steady value quickly. Therefore, the sensitization of CdS on the ITO/TiO_2 film effectively improves the initial photoelectronic response of the ITO/TiO_2, prevent the recombination of photogenerated carriers, and finally, change the conveying speciality of the photogenerated charges in the ITO/TiO_2 electrodes.

As discussed above, when CdS was electrodeposited on the ITO/TiO_2 films, a good electro-contact heterojunction was formed between TiO_2 and CdS. Under visible light illumination, the electrons are excited into the CdS conduction band followed by a quick injection into the TiO_2 conduction band. The band-gap match between CdS and TiO_2 can effectively increase the photoelectron–hole separation. Also, the formation of the heterojunctions, together with the I_3^-/I^- electrolyte, strongly decrease the photogenerated carrier recombination. Therefore, the sensitization of CdS for the ITO/TiO_2 film can improve the photoelectrochemistry performance and photoelectric conversion efficiency of the ITO/TiO_2 films.

4. Conclusion

The ITO/TiO_2/CdS composite thin film electrodes were successfully prepared by electrodeposition technique. The CdS nanoparticle uniformly distribute not only on the surface of TiO_2 but also inside the TiO_2 film, which lead to the formation of an ITO/TiO_2/CdS film with a spatial network CdS particle distribution. The results obtained from the photocurrent-potential behavior and photocurrent action spectra indicated that the sensibilization of narrow-band-gap CdS on broad-band-gap TiO_2 expands the photoabsorption range and makes the threshold value of the photoelectric response have an obvious red shift. Furthermore, CdS can accelerate the transfer of the photogenerated electrons and restrain the combination of carriers. Therefore, the sensibilization of CdS on ITO/TiO_2 can effectively improve the photoelectric conversion efficiency of the ITO/TiO_2 film.

Acknowledgement

This work was supported by the National Natural Science Foundation of China (Nos. 20676027, 20431030, and 20671032) and the Natural Science Foundation of Heilongjiang Province of China (ZJG0602-01).

References

[1] B. O'Regan, J. Moser, M. Anderson, M. Graetzel, J. Phys. Chem. 94 (1990) 8720.
[2] P.A. Sant, P.V. Kamat, Phys. Chem. Chem. Phys. 4 (2002) 198.
[3] C. Nasr, P.V. Kamat, S. Hotchandani, J. Phys. Chem. B 102 (1998) 10047.
[4] R. Vogel, P. Hoyer, H. Weller, J. Phys. Chem. 98 (1994) 3183.
[5] R.S. Singh, V.K. Rangari, S. Sanagapalli, V. Jayaraman, S. Mahendra, V.P. Singh, Sol. Energy Mater. Sol. Cells 82 (2004) 315.
[6] Y.J. Hsu, S.Y. Lu, Langmuir 20 (2004) 194.
[7] L.M. Peter, D.J. Riley, E.J. Tull, K.G.U. Wijayantha, Chem. Commun. (2002) 1030.
[8] K. Yamaguchi, T. Yoshida, T. Sugiura, H. Minoura, J. Phys. Chem. B 102 (1998) 9677.
[9] R. Vogel, K. Pohl, H. Weller, Chem. Phys. Lett. 174 (1990) 241.
[10] S. Kohtani, A. Kudo, T. Sakata, Chem. Phys. Lett. 206 (1993) 166.
[11] R. Flood, B. Enright, M. Allen, S. Barry, A. Dalton, H. Doyle, D. Tynan, D. Fitzmaurice, Sol. Energy Mater. Sol. Cells 39 (1995) 83.
[12] Y.G. Guo, J.S. Hu, H.P. Liang, L.J. Wan, C.L. Bai, Adv. Funct. Mater. 15 (2005) 196.
[13] S.G. Hickey, D.J. Riley, E.J. Tuhh, J. Phys. Chem. B 104 (2000) 7623.
[14] S. Drouard, S.G. Hickey, D.J. Riley, Chem. Commun. (1999) 67.
[15] G.A. Il'chuk, V.O. Ukrainets, Y.V. Rud', O.I. Kuntyi, N.A. Ukrainets, B.A. Lukiyanets, R.Y. Petrus, Tech. Phys. Lett. 30 (2004) 628.
[16] A.V. Feitosa, M.A.R. Miranda, J.M. Sasaki, M.A. Araujo-Silva, Braz. J. Phys. 34 (2004) 656.
[17] E.C. Hao, B. Yang, J.H. Zhang, X. Zhang, J.Q. Sun, J.C. Shen, J. Mater. Chem. 8 (1998) 1327.
[18] D. Robert, Catal. Today 122 (2007) 20.
[19] C.Y. Wang, H.M. Shang, Y. Tao, T.S. Yuan, G.W. Zhang, Sep. Purif. Technol. 32 (2003) 357.
[20] X.M. Qian, D.Q. Qin, Y.B. Bai, T.J. Li, X.Y. Tang, E.K. Wang, S.J. Dong, J. Solid State Electrochem. 5 (2001) 562.
[21] X.M. Qian, D.Q. Qin, Q. Song, Y.B. Bai, T.J. Li, X.Y. Tang, E.K. Wang, S.J. Dong, Thin Solid Films 385 (2001) 152.
[22] R.S. Mane, M.Y. Yoon, H. Chung, S.H. Han, Solar Energy 81 (2007) 290.
[23] M.G. Kang, H.E. Han, K.J. Kim, J. Photochem. Photobiol. A: Chem. 125 (1999) 119.
[24] S. Juodkazis, E. Bernstein, J.C. Plenet, C. Bovier, J. Dumas, J. Mugnier, J.V. Vaitkus, Thin Solid Films 322 (1998) 238.
[25] G.C. Morris, R. Vanderveen, Sol. Energy Mater. Sol. Cells 26 (1992) 217.
[26] D.S. Albin, Y. Yan, M.M. Al-Jassim, Prog. Photovolt: Res. Appl. 10 (2002) 309.
[27] J. Nishino, S. Chatani, Y. Uotani, Y. Nosaka, J. Electroanal. Chem. 473 (1999) 217.
[28] G. Sasikala, R. Dhanasekaran, C. Subramanian, Thin Solid Films 302 (1997) 71.
[29] S. Chen, M. Paulose, C. Ruan, G.K. Mor, O.K. Varghese, D. Kouzoudis, C.A. Grimes, J. Photochem. Photobiol. A: Chem. 177 (2006) 177.
[30] H.M. Cheng, J.M. Ma, Z.G. Zhao, L.M. Qi, Chem. Mater. 7 (1995) 663.
[31] A. Matsuda, Y. Kotani, T. Kogure, M. Tatsumisago, T. Minami, J. Am. Ceram. Soc. 83 (2000) 229.
[32] Q.L. Zhang, D.J. Wang, X. Wei, T.F. Xie, Z.H. Li, Y.H. Lin, M. Yang, Thin Solid Films 491 (2005) 242.
[33] L.Q. Jing, B.F. Xin, F.L. Yuan, L.P. Xue, B.Q. Wang, H.G. Fu, J. Phys. Chem. B 110 (2006) 17860.
[34] In the photochemical processes, the redox couple iodide/tri-iodide is very important. The photo and counter electrodes are exposed to the electrolyte in experiments. After the electrons of semiconductor are excited upon illumination, the photogenerated electrons can quickly be injected into conduction band of another semiconductor followed by a charge separation, resulting in the transport of the photogenerated electrons into external circuit and the concentration of holes in the excited semiconductor. The concentrated holes can be reduced by the substance I^- on the excited semiconductor surface leading to the combination of holes and the formation of I_2 while at the counter electrode the photogenerated electrons can react with I_3^- to form I^-. Therefore, upon illumination, the photocurrent can constantly proceed through the redox couple I^-/I_3^-, as illustrated in Fig. 6.
[35] W.W. So, K.J. Kim, S.J. Moon, Inter. J. Hydrogen Energy 29 (2004) 229.
[36] Y.Q. Wang, H.M. Cheng, Y.Z. Hao, J.M. Ma, W.H. Li, S.M. Cai, Thin Solid Films 349 (1999) 120.
[37] S.M. Yang, C.H. Huang, J. Zhai, Z.S. Wang, L. Jiang, J. Mater. Chem. 12 (2002) 1459.